NMR characterization of obscurinervine and obscurinervidine using novel computerized analysis techniques

James K. Harper,[a] Reinhard Dunkel,[a] Steven G. Wood,[b] Noel L. Owen,[c] Du Li,[c] Rex G. Cates[b] and David M. Grant*,[a]

[a] *Department of Chemistry, University of Utah, Salt Lake City, Utah 84112, USA*
[b] *Department of Botany and Range Science, Brigham Young University, Provo, Utah 84602, USA*
[c] *Department of Chemistry and Biochemistry, Brigham Young University, Provo, Utah 84602, USA*

The ^{13}C and ^{1}H resonances of the alkaloids, obscurinervine (1) and obscurinervidine (2), are assigned using high-field NMR experiments and computerized data analysis procedures. A 2D INADEQUATE analysis of 26 mg of 2 was performed with a high-sensitivity carbon probe and the data interpreted using the spectral analysis program, CCBOND, to provide unambiguous ^{13}C assignments. Although all signals are visually undetectable, CCBOND determined 20 of the 22 carbon–carbon bonds present. Corresponding ^{1}H chemical shift assignments are made from HETCOR data. Proton–proton couplings are determined from DQF-COSY data using the new analysis program, HHCORR. Since HHCORR models signals as AB spin systems, the determined coupling constants are fairly independent of higher order effects, linewidths and digital resolution. Also a significant sensitivity improvement over visual interpretation of DQF-COSY data is observed. The obtained coupling constants are interpreted through the Karplus relationship to provide conformational details. These novel software analysis techniques allow accurate and more routine analysis of INADEQUATE and DQF-COSY data providing non-specialists access to these powerful experiments. Absolute stereochemistry of 2 is determined by a comparison with the ORD curve of (−)-*O*-methylaspidolimine. Stereospecific ^{1}H assignments are obtained from proton–proton couplings and molecular mechanics simulations. The ^{13}C and ^{1}H chemical shift assignments for the related alkaloid, obscurinervine 1, are determined from CCBOND processed 2D INADEQUATE, HHCORR processed DQF-COSY, and HETCOR data. Differences in the rigidity of 1 and 2 in dimethyl sulfoxide (DMSO) are quantified by variable-temperature ^{1}H NMR spectroscopy. Complete conformations of all ring systems are obtained from molecular mechanics using dihedral angles derived from proton–proton couplings as a check on the quality of the model. All conformational conclusions are independently supported by the X-ray structure of 1.

Introduction

Aspidosperma-type alkaloids have been the focus of NMR studies since the early 1960s. This interest has resulted in the characterization of over 170 structures of this class.[1] However, many of these studies were completed before the availability of modern NMR techniques. As a result, no high resolution NMR results are available for most aspidosperma alkaloids. This is especially true for ^{13}C NMR spectroscopy where less than 15% of the known structures have established ^{13}C assignments.[1]

Recently two alkaloids of this type, obscurinervine (**1**) and obscurinervidine (**2**), were isolated and identified as part of our study of Panamanian plants,[2] see Fig. 1. While the X-ray structure for **1**[2] and its hydrobromide salt[3] have been previously described, no high field ^{1}H or complete ^{13}C NMR assignments have been reported.[2,4] Since solution and crystalline structures may differ, a complete NMR characterization of these alkaloids is essential for future structure/function studies. We report here the complete NMR characterization of these compounds.

As part of our characterization, two NMR spectral interpretation programs are used. The first program, CCBOND,[5,6] is designed to establish carbon connectivity from 2D INADEQUATE ^{13}C–^{13}C coupling data with greatly increased sensitivity.[5] To increase further the sensitivity, the data obtained for **2** were acquired on a carbon probe designed specifically for the analysis of small quantities of material.[7] The second program, HHCORR, is a modification of the CCBOND

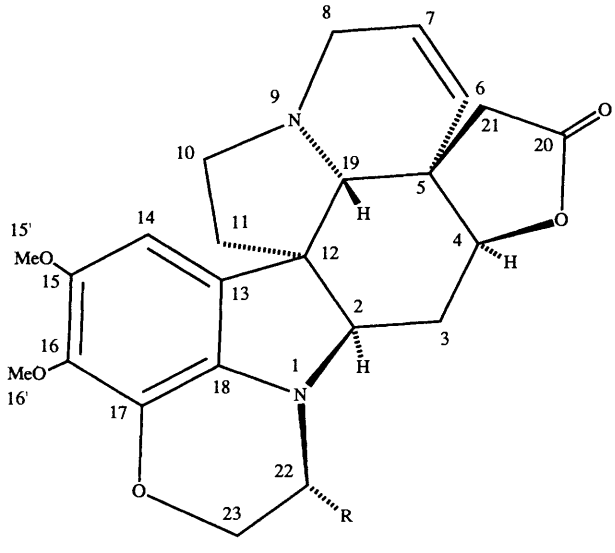

24 25
Obscurinervine (**1**) R = CH_2CH_3

25
Obscurinervidine (**2**) R = CH_3

Fig. 1 Structure of obscurinervine and obscurinervidine showing *Chem. Abstr.* numbering of ring atoms

software for the analysis of phase-sensitive double quantum filtered correlation spectroscopy (DQF-COSY) data. This program provides a significant improvement over visual interpretation for accurately determining proton–proton coupling constants. Conventional NMR experiments are used to provide the remaining assignments to complete the characterization of these alkaloids.

The programs, CCBOND and HHCORR, provide the means to analyse routinely and accurately NMR data which have been difficult or impossible to interpret by other means. This is particularly important for 2D INADEQUATE spectra where the inherent low sensitivity has limited the use of this powerful structure elucidation technique. Since the INADEQUATE pulse sequence allows for the direct determination of carbon skeletons, more widespread use would make structure elucidation of organic molecules more routine and unambiguous. The program CCBOND greatly alleviates sensitivity problems and allows realization of the potential of the INADEQUATE approach.

Complementing the INADEQUATE technique is the DQF-COSY experiment. This method provides, through proton–proton couplings, connectivity information and allows the determination of molecular geometry using the Karplus relationship. However, the results of this experiment are often difficult to interpret owing to the typical under-digitization of 2D NMR data sets and the problems caused by broad lines. The program HHCORR models coupling constants accounting for the mutual signal interference and enhances analysis sensitivity. Thus accurate coupling constants can be obtained even from underdigitized low signal-to-noise data sets. Together, these programs allow non-specialists to determine the structure and geometry of molecules.

The described experiments assign all ^{13}C chemical shifts for these alkaloids and establish three previously unresolved assignments.[2a] The corresponding ^{1}H chemical shifts are obtained from HETCOR data. With all assignments made, conformations and ring inversion barriers are determined.

We report here a complete conformational analysis of both **1** and **2** using HHCORR derived proton–proton couplings and molecular mechanics. In addition, ring inversion barriers for the oxazine and cyclohexane portions of both alkaloids are obtained from variable temperature studies. These studies reveal a surprisingly rigid ethyl side chain in **1**. The rotation barrier and conformation for the ethyl group are included. This rigidity is significant since these alkaloids differ *only* for the substituent at C-22 and this difference corresponds to a significant difference in the oxazine ring flexibility.

Results and discussion

INADEQUATE analysis and chemical shift assignments

The INADEQUATE pulse sequence is designed to detect couplings between ^{13}C pairs.[8] Since most organic molecules have extensive carbon skeletons, this experiment is extremely powerful for structure determination. However, in spite of its immense potential, there has been a reluctance to use this experiment largely due to its inherent insensitivity. Typically, several hundred milligrams of sample are required[9] to provide a sufficient number of adjacent ^{13}C nuclei for natural abundance (1.1%) samples. Furthermore, acquisitions times of 10–50 h are required,[9] and a carbon–carbon coupling constant (J_{CC}) similar to those to be observed must be provided as an input parameter during the experimental set-up. When material is scarce or a compound exhibits a broad range of carbon–carbon coupling constants, it is often difficult to detect all C–C bonds from a single spectrum. For many samples, it is common to encounter both problems simultaneously.

Recently, carbon probes designed specifically for the analysis of small quantities of material have been developed which are well suited for the 2D INADEQUATE experiment.[7] In addition, software for interpreting 2D INADEQUATE spectra which are too noisy for visual assignment has become available.[5] This software has previously allowed analyses of less than 100 μmol of sample when long acquisition times (6–15 days) were used.[5,10,11] In order to test the usefulness of the new probe used in conjunction with the software, **2** was subjected to a 2D INADEQUATE analysis using Varian's carbon nanoprobe for the data acquisition and the CCBOND software for the analysis. This alkaloid exhibits a wide range of carbon–carbon coupling constants, a large number of non-protonated carbons, and quadrupolar nuclei adjacent to carbons, and so provided a rigorous test of this new analysis combination.

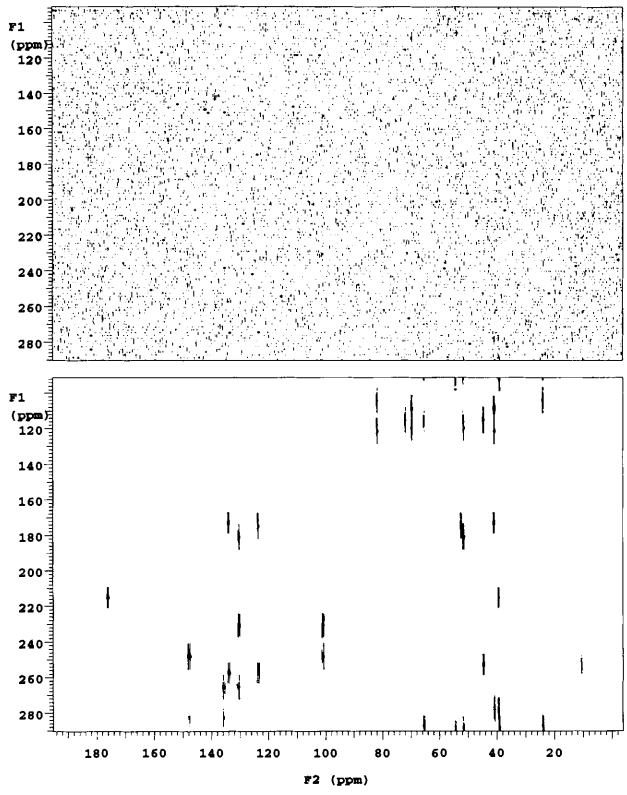

Fig. 2 Comparison of the 2D INADEQUATE data from obscurinervidine (**2**) processed by standard techniques (top) and simulated by CCBOND (see ref. 6) from the analysis results (bottom). Optimal phase parameters determined by CCBOND were used to process the experimental data. The experimental signals barely observable in the upper right quadrant of the experimental data are only visible after applying the phasing obtained through CCBOND.

A 2D INADEQUATE analysis was run on 26 mg of **2** for 63 h using the Varian nanoprobe with a set coupling constant of 65 Hz. The resulting data were processed with the CCBOND software. The software detected 20 of the 22 carbon–carbon bonds. The two bonds not detected (between carbons 13–18 and 17–18) are bonds to the same carbon. Therefore, this carbon is assigned by default. Of the 20 bonds found, all were impossible to detect visually but were detected at greater than 99.5% certainty by the software. Fig. 2 shows a comparison of the experimental 2D INADEQUATE spectrum obtained using standard processing (without the use of linear prediction, zero filling, or weighting functions) with the spectrum calculated by CCBOND from the spectral analysis results.

Complete connectivity in the molecular framework could not be established from this analysis owing to the presence of heteroatoms. However, X-ray analysis had previously established the structure of **1**.[2a,3] Compound **2** differs from **1** only by the presence of a methyl at C-22 rather than an ethyl group. Therefore, comparison with the X-ray structure of **1** established the heteroatom positions and provided most ^{13}C assignments

Table 1 NMR results for obscurinervidine (**2**)

Carbon number	δ_C[a]	δ_H from HETCOR[b]	Proton–proton coupling from 1D ^{1}H spectrum[c]	Proton–proton coupling from HHCORR interpretation of DQF-COSY[c]	Carbon–carbon coupling constants from 2D INADEQUATE[d]
2	65.31	3.28s	$J_{2,3}$ = —, —	$J_{2,3}$ = 4.3, 6.2	$J_{2,3}$ = 38.0 $J_{2,12}$ = 36.0
3	23.85	2.22m 2.38m	$J_{3,3}$ = —	$J_{3,3}$ = 15.4	$J_{3,4}$ = 37.3
4	81.81	4.55d	$J_{3,4}$ = —, 5.0	$J_{3,4}$ = —, 6.0	$J_{4,5}$ = 36.0
5	40.78				$J_{5,6}$ = 42.0 $J_{5,19}$ = 39.8 $J_{5,21}$ = 35.4
6	133.87	5.73s	$J_{6,7}$ = —	$J_{6,7}$ = —	$J_{6,7}$ = 61.7
7	123.56	5.72s	$J_{7,8}$ = —	$J_{7,8}$ = —	$J_{7,8}$ = 42.7
8	52.30	2.73d, *pro-S* 3.46d, *pro-R*	$J_{8,8}$ = 16.1	$J_{8,8}$ = 16.3	
10	54.31	2.35m, *pro-R* 3.24m, *pro-S*	$J_{10,10}$ = — $J_{10,11}$ = —, —	$J_{10,10}$ = 11.4 $J_{10,11}$ = 8.9, 3.7	$J_{10,11}$ = 34.1
11	39.01	1.81m, *pro-R* 2.31m, *pro-S*	$J_{11,11}$ = —	$J_{11,11}$ = 14.6	$J_{11,12}$ = 35.7
12	51.52				$J_{12,13}$ = 44.7 $J_{12,19}$ = 35.7
13	130.29				$J_{13,14}$ = 66.4 $J_{13,18}$ = —
14	100.87	6.35s			$J_{14,15}$ = 70.7
15	147.84				$J_{15,16}$ = 59.0
15′	57.50	3.82s			
16	135.54				$J_{16,17}$ = 66.2
16′	60.72	3.89s			
17	130.51				$J_{17,18}$ = —
18	136.97				
19	69.62	2.32s			
20	176.12				$J_{20,21}$ = 51.6
21	39.26	2.09d, *pro-S* 2.53d, *pro-R*	$J_{20,20}$ = 18.6	$J_{20,20}$ = 18.6	
22	44.60	3.48t	$J_{22,23}$ = 1.8, 1.4 $J_{22,25}$ = 6.7	$J_{22,23}$ = —, — $J_{22,25}$ = 6.6	$J_{22,23}$ = 35.4 $J_{22,25}$ = 35.7
23	71.86	4.15d, *pro-R* 4.21dd, *pro-S*	$J_{23,23}$ = 11.1	$J_{23,23}$ = 10.9	
25	10.43	1.07d			

[a] All ^{13}C chemical shifts were measured in CD_2Cl_2. [b] The following symbols are used: s = singlet, d = doublet, dd = doublet of doublets, t = triplet, m = multiplet. The prochirality of the protons is listed as *pro-R* or *pro-S*. The chemical shift of split signals is reported for the centre of the splitting pattern. The ^{1}H chemical shifts were measured in $CDCl_3$. [c] $J_{X,Y}$ = is used for proton–proton coupling data with the numbers of the carbons holding the coupled protons listed in place of *X*, *Y*. All reported couplings are in Hz. Undetected couplings are designated by —. Undetected couplings are those for which spectral complexity obscured the coupling or where the coupling was less than twice the digital resolution and hence undetectable. [d] The *J* values listed are the one-bond carbon–carbon couplings found by CCBOND. Undetected couplings are designated by —.

for **2**. Long-range HETCOR results allowed for assignment of the final two methoxy carbons[2a] thus completing the assignments. Complete ^{13}C assignments for **2** are given in Table 1.

Complete ^{13}C assignments for **1** were obtained from a CCBOND processed 2D INADEQUATE spectrum using 49 mg of compound and a conventional 5 mm probe. The corresponding ^{1}H chemical shifts for both alkaloids were obtained from HETCOR data. Complete assignments are shown in Tables 1 and 2.

Our analysis indicates the nanoprobe is significantly more sensitive than a conventional probe. In addition, this probe allows the use of shorter pulses than a conventional probe. Short pulses eliminate the need for composite pulses which are frequently used with conventional probes to cover the full spectral width[12] at the expense of decreased sensitivity in the data acquisition.

Another comparison can be made from the 2D INADEQUATE spectrum acquired on the carbon nanoprobe using the coupling constant set to 65 Hz and the 5 mm probe using a set coupling constant of 48 Hz. Using the 65 Hz dataset, which is optimized for detection of sp^2–sp^2 bonds (J_{CC} = 50–80 Hz), the sp^2–sp^3, and sp^3–sp^3 bonded carbons are found, respectively, to have 10% and 15% higher average determined intensity precision[5a] than those in sp^2–sp^2 bonds. The apparent reason is that bonds with lower coupling constants (such as sp^3–sp^3 bonds) typically involve carbons which carry more hydrogens and thus experience improved NOE enhancements. In contrast, when the coupling constant is set to the lower value of 48 Hz, the carbons in the sp^3–sp^3 and sp^3–sp^2 bonds are found, respectively, to be 50% and 120% more intense on average than in the sp^2–sp^2 bonds. This sensitivity difference can cause sp^2–sp^2 bonds to remain undetected. Therefore, the coupling constant should be set for sp^2–sp^2 bonds when such bonds are suspected to be present.

While the carbon nanoprobe improves the sensitivity of the data acquisition, the improved data analysis sensitivity of CCBOND is crucial since none of obscurinervidine's bonds are visible using standard processing of the 2D INADEQUATE data. The combination of nanoprobe and CCBOND software offers a powerful new approach to the 2D INADEQUATE analysis. More importantly, this combination lowers the required amount of material and spectrometer time to a level approaching a routine analysis. This path is extremely desirable owing to the unparalleled confidence ^{13}C chemical shift assignments from 2D INADEQUATE carry.

Absolute stereochemistry

The absolute stereochemistry of both molecules is needed in order to provide stereospecific ^{1}H assignments. Relative

Table 2 NMR results for obscurinervine (**1**)

Carbon number	δ_C[a]	δ_H from HETCOR[b]	Proton–proton coupling from 1D ^{1}H spectrum[c]	Proton–proton coupling from HHCORR interpretation of DQF-COSY[c]	NOESY[d]	ROESY[d]	Carbon–carbon coupling constants from 2D INADEQUATE[e]
2	64.58	3.41s	$J_{2,3}$ = —, —	$J_{2,3}$ = 2.3, 3.5	1.79	1.79, 2.36, 1.60	$J_{2,3}$ = 38.1 $J_{2,12}$ = 36.0
3	23.54	2.22m 2.36m	$J_{3,3}$ = —	$J_{3,3}$ = 15.1			$J_{3,4}$ = 37.3
4	81.58	4.55d	$J_{3,4}$ = —, 4.7	$J_{3,4}$ = —, 4.9			$J_{4,5}$ = 39.0
5	40.57						$J_{5,6}$ = 41.9 $J_{5,19}$ = 40.0 $J_{5,21}$ = 35.5
6	133.57	5.72s	$J_{6,7}$ = —	$J_{6,7}$ = —	2.09		$J_{6,7}$ = 70.3
7	123.34	5.72s	$J_{7,8}$ = —, 2.7	$J_{7,8}$ = 1.7, 2.4			$J_{7,8}$ = 41.8
8	52.11	2.72d, *pro-S* 3.47d, *pro-R*	$J_{8,8}$ = 16.3	$J_{8,8}$ = 16.3			
10	54.19	2.38m, *pro-R* 3.24m, *pro-S*	$J_{10,10}$ = — $J_{10,11}$ = —, —	$J_{10,10}$ = 14.1 $J_{10,11}$ = 7.3, 7.2		2.38, 3.41	$J_{10,11}$ = 34.6
11	38.89	1.79m, *pro-R* 2.28m, *pro-S*	$J_{11,11}$ = —	$J_{11,11}$ = 16.5	1.79, 3.41	1.79, 3.41	$J_{11,12}$ = 35.6
12	51.24						$J_{12,13}$ = 43.9 $J_{12,19}$ = 35.5
13	129.33						$J_{13,14}$ = 67.3 $J_{13,18}$ = —
14	100.32	6.34s				3.82	$J_{14,15}$ = 70.3
15	147.28						$J_{15,16}$ = —
15′	57.38	3.82s				6.34	
16	135.66						$J_{16,17}$ = —
16′	60.90	3.88s					
17	130.83						$J_{17,18}$ = —
18	136.80						
19	69.47	2.33s					
20	176.29						$J_{20,21}$ = 51.2
21	39.08	2.09d, *pro-S* 2.53d, *pro-R*	$J_{20,20}$ = 18.6	$J_{20,20}$ = 18.6	2.09, 5.72		
22	50.49	3.19dt	$J_{22,23}$ = 1.5, 1.7 $J_{22,25}$ = —, 10.0	$J_{22,23}$ = —, — $J_{22,25}$ = 4.0, 10.5			$J_{22,23}$ = 35.8 $J_{22,24}$ = 35.5
23	67.79	4.08d, *pro-R* 4.38dd, *pro-S*	$J_{23,23}$ = 11.4	$J_{23,23}$ = 11.3			
24	16.78	1.34m, *pro-R* 1.60m, *pro-S*	$J_{24,24}$ = — $J_{24,25}$ = 7.5	$J_{24,24}$ = 16.2 $J_{24,25}$ = 7.7		1.60, 3.41	$J_{24,25}$ = 34.4
25	10.28	0.98t					

[a] All ^{13}C Chemical shifts were measured in CD_2Cl_2. [b] The following symbols are used: s = singlet, d = doublet, dd = doublet ofdoublets, dt = doublet of triplets, t = triplet. The prochirality of the protons are listed as *pro-R* or *pro-S*. The chemical shifts of split signals are reported for the centre of the splitting pattern. The ^{1}H chemical shifts were measured in $CDCl_3$. [c] $J_{X,Y}$ = is used for proton–proton coupling data with the numbers of the carbons holding the coupled protons listed in place of *X*, *Y*. All reported couplings are in Hz. Undetected couplings are designated by —. Undetected couplings are those for which spectral complexity obscured the coupling or where the coupling was less than twice the digital resolution and hence undetectable. [d] For the ROESY and NOESY experiments, interactions between hydrogens on the same carbon were not included in the table. The values in these columns identify the chemical shifts of the interacting hydrogen. [e] The *J* values listed are the one-bond carbon–carbon couplings found by CCBOND. Undetected couplings are designated by —.

stereochemistry of **1** was established by X-ray analysis[2] and matched previously reported results.[3] The optical rotation of **1** and **2** also matched those reported by Brown, establishing that these alkaloids have the same absolute stereochemistry as previously described.[4] Brown's ORD curves for both alkaloids[4] were found closely to match the curve of the related compound (−)-*O*-methylaspidolimine[13] for which the absolute stereochemistry is known. This comparison establishes the absolute stereochemistry of **1** and **2** to be 2*R*, 4*S*, 5*R*, 12*R*, 19*S*, 22*R*. The rigidity of these compounds appears also to make the nitrogens chiral. This is reflected in the proton spectrum where protons attached to carbons next to nitrogens are anisotropic as expected for a rigid structure. Based on X-ray results, the assignments for the nitrogens are 1*S* and 9*S*.

These assignments also establish the absolute stereochemistry for the related alkaloid neblinine, and the 6,7-dihydro derivatives of **1** and **2** which were reported by Klyne to have the same absolute stereochemistry as reported for obscurinervine.[14] With the absolute stereochemistry established, stereospecific assignments of all protons were made.

HHCORR analysis of DQF-COSY data

To obtain stereochemical proton assignments and conformations in solution, accurate proton–proton coupling constants are needed. These couplings may be determined from DQF-COSY data or from a variety of other methods[15–21] using unique processing techniques. However, accurate visual coupling constant determination usually requires enormous data sets, while alternative processing methods typically have difficulty dealing with low signal-to-noise and may require acquisition of more than one type of experimental data. The program HHCORR, developed for the analysis of DQF-COSY data sets, addresses these problems.

The HHCORR software examines all four phase-quadrants of phase-sensitive data. The software models the experimental signals as AB spin systems using an equation which includes a coupling constant and two chemical shift parameters. The best-fit values of these spectral parameters are obtained from regression analysis of the experimental signals. Based upon the non-linear regression error values,[5c] intensity parameter precision values are calculated and used to determine the

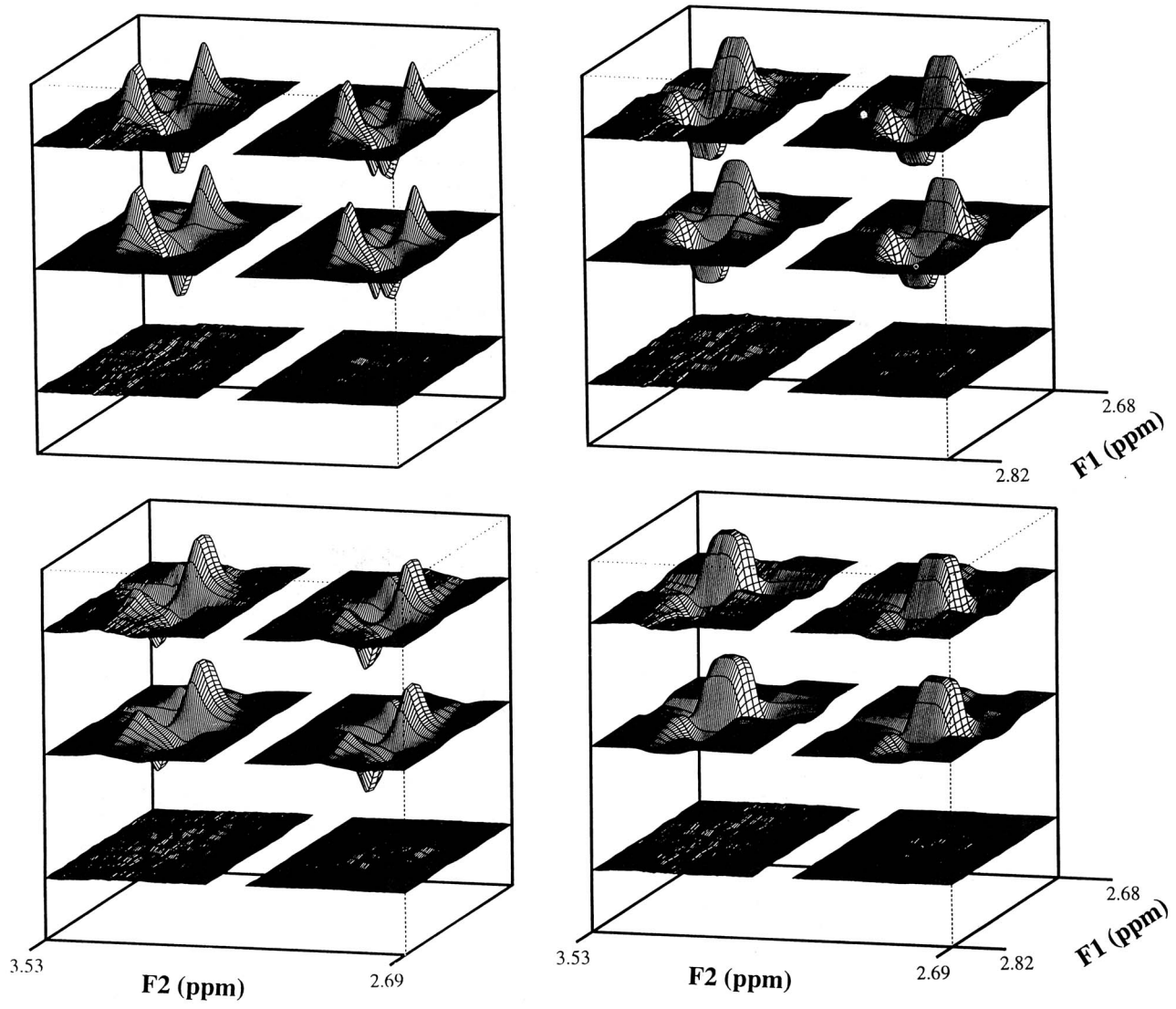

Fig. 3 DQF-COSY correlation signal for the geminal protons on C-8 in **2**. The subfigures show the auto-phased off-diagonal transitions in all four phase quadrants. Each subfigure shows from top to bottom: the experimental, simulated and residual spectral areas. The shown *F*1 numbering corresponds to the low-frequency off-diagonal signal shown on the left side of each subfigure.

probability that the analysed signal is a genuine correlation signal.[5a] This approach is comparable to the analysis performed by CCBOND, therefore the advantages found for HHCORR are similar to those of CCBOND, namely, increased sensitivity over visual interpretation, the ability to process unphased data, to determine accurately AB couplings, and to distinguish noise spikes and solvent ridges from genuine signals. However, in contrast with CCBOND, the smaller frequency range of protons, the increased width of a correlation signal in the *F*1 dimension, and the complexity introduced by passive couplings (see below) greatly increase the challenges posed by unresolved or even destructive signal overlap for the HHCORR analysis.

The increased sensitivity of the automated analysis compared with the visual interpretation partly arises from the simultaneous modelling of the signals in all four quadrants of the hypercomplex data set. The visual interpretation is limited to one phase quadrant and therefore ignores available information. This additional sensitivity allows the accurate analysis of higher molecular weight samples or of smaller amounts of lower molecular weight materials. In addition, HHCORR works with unphased data and determines proper phase functions from phase parameter values derived from spectral correlation signals.[22] These phase functions are more accurate than those obtainable from traditional phasing methods.

In contrast with peak-picking algorithms frequently used in computerized evaluation of 2D data sets, HHCORR explicitly evaluates the fine structure of active couplings in DQF-COSY spectra. HHCORR models a correlation signal as the sum of anti-phase AB spin transitions rendering the determined coupling constants insensitive to partial signal cancellation[23] encountered whenever the linewidths approach the coupling constants. The HHCORR modelling includes sinc lineshape convolutions caused by finite acquisition times. This allows the software to be less sensitive to low digital resolution and widely different digital resolution in both spectral dimensions. Finally, the highly constrained spin system model, fitted simultaneously to all four phase quadrants, provides a powerful filter to prevent experimental artifacts in the spectrum from being misinterpreted as correlation signals.

The HHCORR program still needs to be speed optimized as a thorough analysis of the 90 MByte DQF-COSY dataset of **2** took several hours on an IBM RS/6000-370 workstation. Fig. 3 shows the strongest active coupling signal found during the analysis, the 16.25 ± 0.01 Hz geminal coupling of the protons on C-8. The subfigures show the four phase quadrants of the bond signal after auto-phasing. Each subfigure shows from top to bottom: the experimental, simulated and residual signal. The model equation can explain 99.1% of the signal power in all phase quadrants of the spectral region. The encountered 0.9% difference is likely due to an unresolved vicinal coupling to the proton on C-8 and experimental lineshape distortions caused by magnet inhomogeneity.

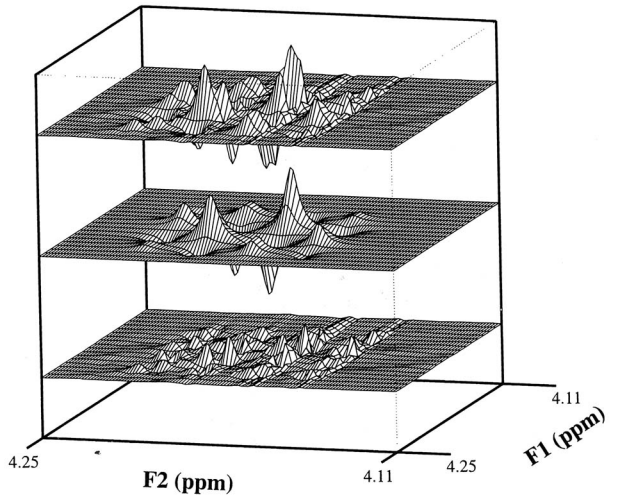

Fig. 4 DQF-COSY absorption mode signals of the 10.9 Hz geminal coupling of the C-23 protons in **2**. From top to bottom are shown the experimental, simulated and residual spectral area. The simulated spectral area includes all 16 transitions and correctly models the higher order effects of this spin system. The shown residuals are caused by an unresolved passive coupling of the C-23 protons to the vicinal C-22 proton and by the overlapping diagonal signals of a long-range coupling of the C-23 protons to the C-25 methyl group.

HHCORR is based on the quantum mechanical treatment of an AB spin system. Hence accurate coupling constants can be obtained from severe AB correlation signals which are quite uninterpretable visually even if clearly observable. Fig. 4 shows HHCORR's best-fit of the analysis model to the AB spin system created by the two protons on C-23 of **2**. DQF-COSY spectra contain not only active couplings, which appear as anti-phase correlation signals,[23] but also in-phase splittings caused by additional proton couplings to one of the actively coupled spins. The partly resolved passive coupling of the proton on C-22 to both active, coupled geminal protons on C-23 causes the additional splitting in Fig. 4. The diagonal transitions of both the active coupling to the C-22 protons as well as the long-range active coupling to the C-25 methyl protons are contained in the shown experimental signal as well.

HHCORR exclusively determines coupling constants from the active couplings. HHCORR averages out small in-phase passive couplings by increasing the corresponding linewidths during the regression analysis. The coupling constants of passive couplings are obtained elsewhere in the spectrum from the corresponding active couplings. If the active coupling is smaller than a superimposed passive coupling, the correlation signal appears as two separate correlation-patterns as shown in Fig. 5. The active vicinal coupling of the proton on C-2 with one of the C-3 protons in **2** has a superimposed larger passive geminal coupling caused by the second proton on C-3. Averaging out the passive coupling is not possible and HHCORR reports the coupling as two separate patterns as shown on the top and bottom of Fig. 5. Since passive couplings are in-phase while active couplings are anti-phase, misinterpretations of such patterns by HHCORR are unlikely.

The overlap of signals in DQF-COSY spectra can become unduly complex. However, the combination of averaging and reporting separated patterns as distinct coupling patterns normally allows the approximate analysis of otherwise uninterpretable signal correlations. Fig. 6 shows the coupling signals of the 2.35 and 1.81 ppm protons on carbons 10 and 11 in **2**. HHCORR can account for only 72.7% of the observed signal power in the four phase quadrants. However, the determined coupling constant of 8.86 Hz with a marginal standard deviation of ±0.53 Hz is likely more precise than coupling constants determined visually.

HHCORR logically condenses the information of a DQF-

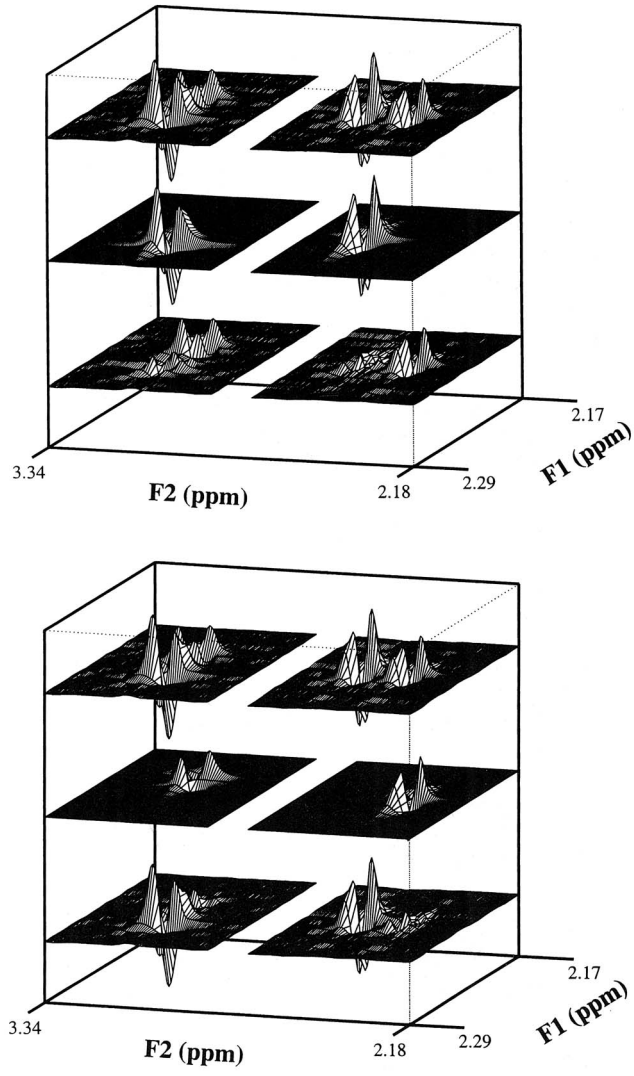

Fig. 5 DQF-COSY absorption mode signal of the 4.3 Hz vicinal coupling of the 3.28 ppm C-2 proton and the 2.22 ppm C-3 proton in **2**. Owing to the baseline resolved additional 15.4 Hz geminal coupling between the C-3 protons, HHCORR detects two distinct correlation signals shown in both subfigures. Each subfigure shows, from top to bottom, the experimental, simulated and residual spectral area. The experimental data in both subfigures are identical. The shown *F*1 numbering corresponds to the low-frequency off-diagonal signal on the left side of the figure.

COSY spectrum to a table of detected correlation signals. This table can then be used for manual or automated structure elucidation or molecular modelling. As visual feedback, HHCORR provides a simulated spectrum matching the analysed experimental data as shown in Fig. 7. The experimental spectrum shown (top) was phase corrected using HHCORR-determined phasing parameters. The phased simulated spectrum is shown at the bottom of the figure. As can be seen, all resolved coupling signals are characterized. However, two correlation signals (at 3.48 and 1.07 ppm) to the strongly coupled protons resonating around 4.2 ppm are not shown in the HHCORR-simulated spectrum since they involve a vicinal and a long-range coupling superimposed on the already complicated AB spin system at 4.2 ppm. The present version of HHCORR cannot yet adequately characterize these correlation signals.

To verify the accuracy and sensitivity of HHCORR, proton–proton couplings for **1** and **2** were obtained from HHCORR processed DQF-COSY data. Where possible, couplings were obtained from both high resolution 1D ^{1}H spectra and manual interpretation of DQF-COSY signals for comparison. A list of couplings found in the 1D ^{1}H spectra and by HHCORR is given in Tables 1 and 2. The HHCORR couplings matched

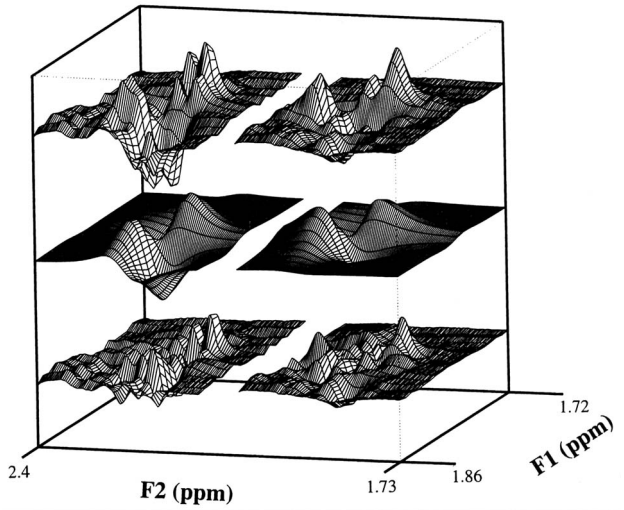

Fig. 6 DQF-COSY absorption mode signals for the vicinal coupling between C-10 and C-11 protons showing, from top to bottom, the experimental, simulated and residual signal in **2**. The overlapping smaller couplings which are barely resolved in the experimental spectrum are averaged out in the spectral simulation. The shown *F*1 numbering corresponds to the low-frequency off-diagonal signal shown on the left side of the figure.

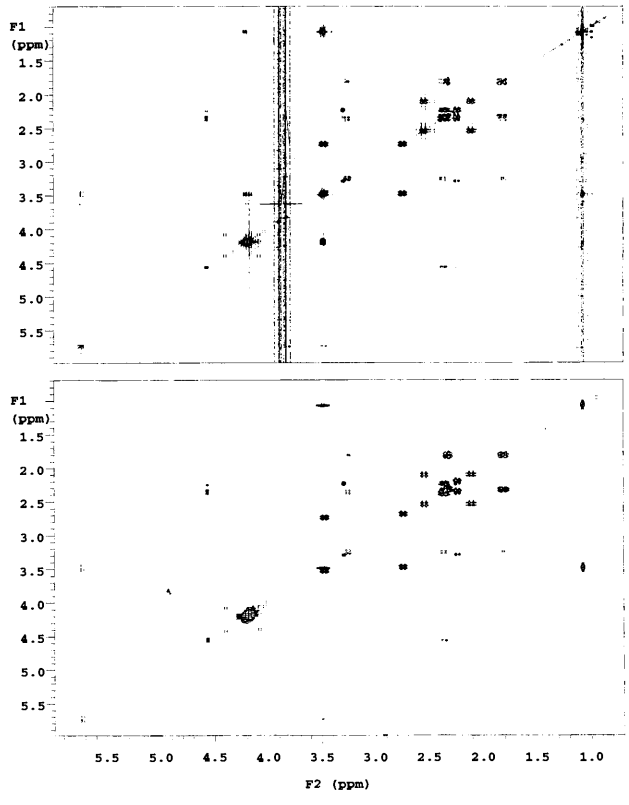

Fig. 7 Comparison of the obscurinervidine (**2**) DQF-COSY spectrum processed by standard techniques (top) and simulated from the spectral analysis results of HHCORR (bottom). Although diagonal signals are not analysed by HHCORR, these resonances can still be simulated from the analysis results and are included in the simulated spectrum to resemble more closely the appearance of the experimental data. The complexity of the correlations between the protons resonating at 3.45 and 1.05 ppm with the signal at 4.2 ppm causes these correlations to be unrecognized by HHCORR. These correlations are not included in the simulated spectrum. The vertical scale of the simulated spectrum is slightly lower than the experimental spectrum to allow all the separation in the *F*1 dimension to be observable.

those found visually to within ±4% for couplings over 2 Hz. For smaller couplings between 1.7 and 2 Hz, HHCORR provided a best-fit average to the poorly resolved fine structure that obscured these couplings. No couplings less than 1.7 Hz

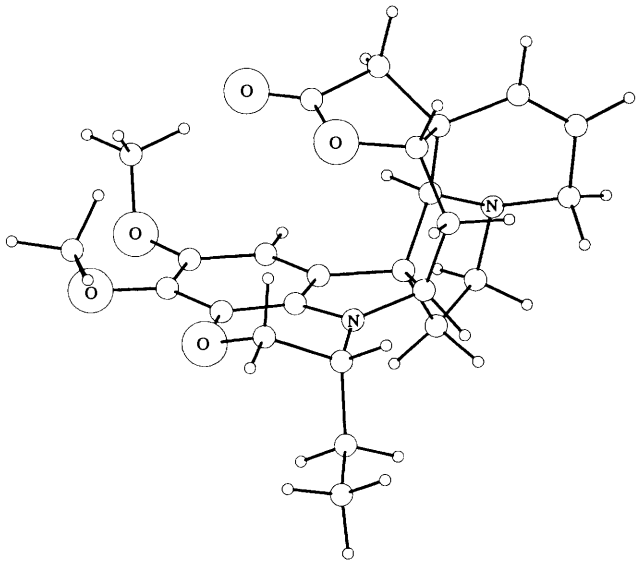

Fig. 8 Molecular mechanics energy-minimized structure for obscurinervine (**1**). The C-24, 25 bond was constrained to remain staggered between the C-22, 23 bond and C-22 proton in agreement with the observed proton–proton couplings.

were determined by HHCORR or by visual interpretation of the DQF-COSY data.

HHCORR determined several couplings that are unobtainable from visual inspection of the DQF-COSY data. Specifically, HHCORR determined six resonances in **2** that are visually uninterpretable owing either to off-diagonal overlap of multiple correlations or to sinc dominated lineshapes.[5a] The DQF-COSY data for **1** were acquired at much lower resolution than the corresponding data for **2**, and accurate correlations were visually unobtainable. Nevertheless, HHCORR determined 16 couplings which matched the values from the high resolution 1D proton spectrum to within ±4% for couplings over 3 Hz.

Stereospecific ^{1}H assignments

Stereospecific assignments for most protons were obtained using a combination of HETCOR, DQF-COSY proton–proton couplings and molecular mechanics simulations. Initially, protons were assigned to specific carbons with HETCOR data. The DQF-COSY experiment was then performed and the data analysed by HHCORR to provide proton–proton couplings. A list of the couplings observed are summarized in Tables 1 and 2.

Stereochemical structures between coupled protons are derived from the Karplus relationship.[24] The dihedral angles predicted from vicinal couplings are summarized in Table 3 together with the angles obtained from the molecular mechanics models. Stereochemical ^{1}H chemical shift assignments of 12 of the 14 prochiral protons on **1** and 10 of the 12 prochiral protons on **2** ensue from these results (see Tables 1 and 2). Prochiral assignments for the protons on C-3 are unattainable for either alkaloid since the protons on both C-2 and C-4 are staggered with respect to the C-3 protons. This causes the magnitude of the coupling between C-2 or C-4 with both protons on C-3 to be nearly identical, yielding no stereochemical information.

Ring system conformations

Compounds **1** and **2** are hydrogen poor. Therefore proton–proton couplings are insufficient to establish ring system conformations. To obtain this information, energy-minimized molecular mechanics models of both alkaloids were generated. In **1**, the ethyl group was constrained to remain at 55° (± 5°) relative to the C-22, 23 bond, as required by the vicinal coupling

Table 3 Conformational predictions of dihedral angles from vicinal proton couplings and corresponding molecular modelling predictions

Protons forming dihedral angle		Dihedral angle from proton couplings/deg		Dihedral angle from molecular modelling/deg	
		1	**2**	**1**	**2**
CH at C-22	*pro-S* at C-23	60	60	67	68
CH at C-22	*pro-R* at C-23	60	60	49	49
CH at C-2	*pro-S* at C-3	50	55	41	43
CH at C-2	*pro-R* at C-3	70	65	75	73
CH at C-4	*pro-S* at C-3	35	75	40	64
CH at C-4	*pro-R* at C-3	85	45	72	51
pro-R at C-10	*pro-S* at C-11	25	47	22	35
pro-R at C-10	*pro-R* at C-11	145	150	148	153
CH at C-22	*pro-S* at C-24	45	—	51	—
CH at C-22	*pro-R* at C-24	165	—	167	—

Table 4 Ring system conformations obtained from molecular modelling and X-ray analysis

Ring system	Observed conformation
Cyclohexane	Twist boat
Indole	Planar
Oxazine	Half twist
Lactone	Near planar
Piperidine	Half twist
Pyrrolidine	Half chair

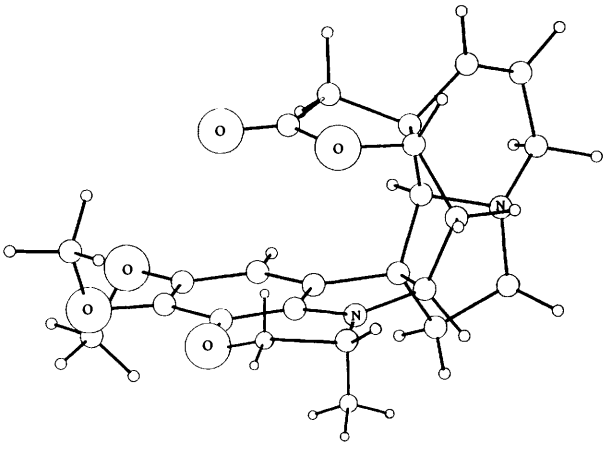

Fig. 9 Molecular mechanics energy-minimized structure for obscurinervidine (**2**). No dihedral constraints were necessary to obtain a structure consistent with the dihedral angles derived from observed proton–proton couplings.

constant between the protons on C-22 and C-24. No constraints were used in the minimization of **2**. The resulting structures are shown in Figs. 8 and 9.

The molecular modelling provided ring conformations that were verified by the dihedral angles obtained from coupling constants. All angles agreed to within ± 15°, indicating a close match between the overall geometry of the minimized model structures and the actual solution structures (see Table 3). Further, all ring conformations predicted from molecular mechanics matched those obtained in the X-ray analysis of solid **1**. This approach offers an alternative to conformational analysis using more difficult studies with long-range CH or CC NMR coupling constants[25] and avoids the more traditional solid methods such as X-ray analysis. The ring conformations are summarized in Table 4. All stereochemical relationships and stereospecific ^{1}H assignments were supported independently by the NOESY and ROESY data from **1**.

Ring inversion data

Compounds **1** and **2** contain unusually constrained oxazine and cyclohexane ring systems. Therefore, these compounds offer an opportunity to obtain reference ring inversion barriers for restricted six-membered rings. Since **1** and **2** differ only at the substituent on the oxazine ring, these results quantify the major conformational difference between these alkaloids in solution. Variable temperature ^{1}H NMR data provide information on the barrier to inversion. Coalescence temperatures of the two C-23 protons were obtained by extrapolating a linear (R^2 > 0.99) plot of temperature *versus* difference in chemical shift. The free energies were then calculated as described by Sutherland[26] (Table 5). This analysis clearly illustrates that this small difference in structure results in a change in flexibility of a significant portion of the structure.

The complete ^{1}H assignments and the high resolution of the data made it possible also to study the inversion of the cyclohexane ring. Conformational studies of cyclohexanes have traditionally been of great interest.[27] Compounds **1** and **2** each have a cyclohexane ring fused on four adjacent sides making it of interest as a model system. Examination of the variable temperature work revealed that these compounds are partially ordered in solution, and the frequency difference of the two protons on C-3 becomes greater rather than coalescing as the temperature increases (see Table 5). This result is explained by the solution becoming more isotropic as the increasing thermal motion destroys the ordering. Consequently, it was impossible to determine the coalescence temperature of the C-3 protons. However, as the tendency to move towards an isotropic solution is much larger than the tendency towards coalescence, it is possible to conclude that the cyclohexane ring must be quite rigid.

Obscurinervine ethyl group rotation

The variable temperature study also allowed determination of the rotation barrier for the ethyl side chain in **1**. The two protons on C-24 yield multiplets at two different chemical shifts rather than the expected multiplet at a single chemical shift. This result is consistent with a non-rotating ethyl side chain. Coalescence data obtained from the variable temperature ^{1}H NMR analysis are summarized in Table 5. This analysis reveals a surprisingly rigid ethyl group.

Ecological significance

Ecologically, the role of alkaloids in secondary plant chemistry has been difficult to assess. Some alkaloids have a specific defensive role but general relationships have not been established.[28] No biological function of the alkaloids studied in this report is presently known.[2] However, they are present in such high concentrations (**1** and **2** account for about 1.6% of the dry weight on the average) that it is likely they provide some benefit to the plant. As this study establishes the structural details of these alkaloids in solution, the structural basis essential for future structure/function relationships has been established.

Table 5 Variable temperature ^{1}H NMR results

	$\Delta\delta$/Hz[b]				
	Cyclohexane ring		Oxazine ring		Ethyl group
T/K[a]	1	2	1	2	1
297	Not measured	Not measured	259	115	228
306	59	60	250	108	222
319	70	78	238	99	214
324	75	79	232	94	208
342	83	87	213	80	195
362	93	95	197	66	185
384	102	103	180	51	172
404	109	109	163	38	164
T_c/K[c]	—	—	593	461	676
K_c/s^{-1}	—	—	575	255	506
ΔG_c/kJ mol^{-1}	—	—	113.6	90.2	135.2

[a] Temperatures below 342 K were determined with respect to a sealed methanol standard. Temperatures above 342 K were determined with respect to a sealed ethylene glycol standard. [b] Chemical shift differences in the oxazine ring were measured only for the geminal protons on C-23. Chemical shift differences in the cyclohexane ring were measured only for the geminal protons of C-3. [c] Coalescence temperature.

Table 6 Parameters used for NMR experiments

	1D ^{13}C	1D ^{1}H	2D INADEQUATE[a]	DQF-COSY	HETCOR	NOESY	ROESY
Obscurinervine (**1**)							
90° pulse width/μs	11.0	12.5	12.9	11.1	11.0	12.5	12.5
Sample amount/mg[b]	40	10	49	10	40	10	10
No. transients per FID	256	128	128	16	16	16	8
Recycle time/s	6	4	13	4	1.5	0.5	0.7
*F*1 spectral width/kHz	—	—	25	4.9	4.5	4.5	4.5
*F*2 spectral width/kHz	22	5	25	4.9	18	4.5	4.5
*F*1 digital resolution/Hz point^{-1}	—	—	49	19.5	17.7	17.5	8.7
*F*2 digital resolution/Hz point^{-1}	0.6	0.2	0.8	0.3	35.0	1	1
Total acquisition time/h	0.1	0.02	170.4	9	3.5	2.3	2.5
Obscurinervidine (**2**)							
90° pulse width/μs	11.0	12.5	4.2	12.1	11.0	—	—
Sample amount/mg[b]	49	10	26	10	49	—	—
No. transients per FID	256	128	128	16	16	—	—
Recycle time/s	6	4	10	1.8	1.5	—	—
*F*1 spectral width/kHz	—	—	25	3.8	4.5	—	—
*F*2 spectral width/kHz	22	4	25	3.8	18	—	—
*F*1 digital resolution/Hz point^{-1}	—	—	284	3.9	17.7	—	—
*F*2 digital resolution/Hz point^{-1}	0.6	0.2	0.8	0.6	35.0	—	—
Total acquisition time/h	0.1	0.02	63	18	3.5	—	—

[a] The 2D INADEQUATE spectrum of **1** was acquired on a conventional 5 mm probe while the corresponding spectrum of **2** was acquired using the Varian carbon nanoprobe. [b] The nanoprobe 2D INADEQUATE analysis was performed with a 35 μl sample volume. All other samples were analysed in a 0.7 cm^3 volume.

Experimental

Isolation and characterization

Complete details of sample collection, isolation of **1** and **2**, X-ray analysis of **1** and physical characterization of **1** and **2** have been reported elsewhere.[2]

Molecular modelling

QUANTA/CHARMM molecular mechanics software was used for all modelling.[29] The minimization was performed using the method of steepest descent which was terminated when the energy value gradient between cycles was less than 0.004 kJ mol^{-1} Å^{-1}. All chiral carbons and nitrogens were stereospecifically assigned before minimization. A minimization for both alkaloids was performed with no structural constraints. Compound **1** was then reminimized with the C-24, 25 bond staggered between the C-22, 23 bond and the proton on C-22, consistent with the observed vicinal proton–proton coupling constant.

NMR analysis parameters

A 2D INADEQUATE experiment was performed with the Varian carbon nanoprobe on a 500 MHz Varian Unity plus spectrometer using 26 mg (61 μmol) of **2** in approximately 35 μl of CD_2Cl_2. The spectrum was referenced by assigning a frequency of 53.8 ppm to the centre line of CD_2Cl_2. The pulse sequence was optimized for the detection of 65 Hz coupling constants. A conventional 2D INADEQUATE analysis was performed on 49 mg of **1** in 0.7 cm^3 $CDCl_3$ with a conventional 5 mm broadband probe and a carbon–carbon coupling constant value set to 48 Hz. The spectrum was referenced to the centre line of $CDCl_3$ at 77.0 ppm. Details of the computerized analysis program, CCBOND, used for 2D INADEQUATE data interpretation have been given elsewhere.[5] All other NMR measurements (excluding the variable temperature experiments) were carried out at 26 °C in 5 mm sample tubes using a Varian VXR-500 spectrometer. Variable temperature experiments were performed using approximately 10 mg of **1** and **2** in DMSO. With the exception of the 2D INADEQUATE experiment acquired using a conventional 5 mm probe, the

pulse sequences provided by the manufacturer were used to obtain all 2D spectra. The conventional 2D INADEQUATE spectrum was acquired using a composite pulse sequence designed to provide better coverage of the spectral width.[12] All ^1H chemical shifts are listed with reference to $SiMe_4$. The ^{13}C chemical shifts (excluding the 2D INADEQUATE analysis in CD_2Cl_2) are listed with reference to the centre line of $CDCl_3$ at 77.0 ppm. All reported J values are given in Hz.

The ROESY (rotating frame NOE) experiment was performed with mixing times of 200 and 400 ms while the NOESY experiment was performed with a mixing time of 100 ms. Heteronuclear correlation (HETCOR) experiments were acquired in absolute value mode and processed using Gaussian apodization. Long range HETCOR results are published elsewhere.[2a] All other NMR acquisition parameters are summarized in Table 6.

Note added in proof: the review by M. Eberstadt, G. Gemmecker, D. F. Mierke and H. Kessler, *Angew. Chem., Int. Ed. Engl.*, 1995, **34**, 1671, provides a good summary of the methods covered in refs. 15–21.

Acknowledgements

Funding for this research was provided by NIH grant GM 08521-34 (to D. M. G.) and NSF grant BSR-8806081 (to R. G. C.). The development of CCBOND and HHCORR was partially funded by NIH through SBIR grants 1R43RR07542-01 and 9R44MH53965-02. We would like to thank Dr Charles L. Mayne for valuable suggestions in the set up and interpretation of the 2D INADEQUATE results. We are grateful to Drs Bai Shi, TiaminWang and Wei Wang for helpful discussions, and to the BYU chemistry department for providing NMR instrument time. We would like to thank Varian and Dr Paul Keifer for access to their facilities and use of their carbon nanoprobe for the 2D INADEQUATE analysis of **2**.

References

1 G. A. Cordell, J. E. Saxton, M. Shamma and G. F. Smith, *Dictionary of Alkaloids*, Chapman and Hall, New York, 1989, vol. 2, pp. 413–444.
2 (*a*) J. K. Harper, N. K. Dalley, N. L. Owen, S. G. Wood and R. G. Cates, *J. Crystallogr. Spectrosc. Res.*, 1993, **23**, 1005; (*b*) J. K. Harper, M.S. Thesis, Brigham Young University, 1993.
3 J. Kahrl, T. Gebreyesus and C. Djerassi, *Tetrahedron Lett.*, 1971, **27**, 2527.
4 K. S. Brown and C. Djerassi, *J. Am. Chem. Soc.*, 1964, **86**, 2451.
5 (*a*) R. Dunkel, C. L. Mayne, R. J. Pugmire and D. M. Grant, *Anal. Chem.*, 1992, **64**, 3133; (*b*) R. Dunkel, C. L. Mayne, M. P. Foster, C. M. Ireland, D. Li, N. L. Owen, R. J. Pugmire and D. M. Grant, *Anal. Chem.*, 1992, **64**, 3150; (*c*) R. Dunkel, C. L. Mayne, J. Curtis, R. J. Pugmire and D. M. Grant, *J. Magn. Reson.*, 1990, **90**, 290; (*d*) R. Dunkel, Ph.D. Thesis, University of Utah, 1990.
6 The program CCBOND is available for IBM RS/6000, SGI and SUN SPARC workstations and currently supports Bruker (Aspect), Felix and Varian VNMR data formats. CCBOND is marketed by Varian Associates, Inc. as part of their Full Reduction of Entire Datasets (FRED™) software package.
7 T. M. Barbara, *J. Magn. Reson. A*, 1994, **109**, 265.
8 A. Bax, R. Freeman and S. P. Kempsell, *J. Am. Chem. Soc.*, 1980, **102**, 4849.
9 J. Buddrus and H. Bauer, *Angew. Chem., Int. Ed. Engl.*, 1987, **26**, 625.
10 M. P. Foster, C. L. Mayne, R. Dunkel, R. J. Pugmire, D. M. Grant, J.-M. Kornprobst, J.-F. Verbist, J.-F. Biard and C. M. Ireland, *J. Am. Chem. Soc.*, 1992, **114**, 1110.
11 P. Perera, R. Andersson, L. Bohlin, C. Andersson, D. Li, N. L. Owen, R. Dunkel, C. L. Mayne, R. J. Pugmire, D. M. Grant and P. A. Cox, *Magn. Reson. Chem.*, 1993, **31**, 472.
12 M. H. Levitt and R. R. Ernst, *Mol. Phys.*, 1983, **50**, 1109.
13 W. Klyne, B. W. Swan, D. Bycroft and H. Schmid, *Helv. Chim. Acta*, 1966, **49**, 833.
14 W. Klyne, B. W. Swan, D. Bycroft, D. Schumann and H. Schmid, *Helv. Chim. Acta*, 1965, **48**, 443.
15 Y. Kim and J. H. Prestegard, *J. Magn. Reson.*, 1989, **84**, 9.
16 (*a*) J. J. Titman and J. Keeler, *J. Magn. Reson.*, 1990, **89**, 640; (*b*) S. Ludvigsen, K. V. Andersen and F. M. Poulsen, *J. Mol. Biol.*, 1991, **217**, 731.
17 (*a*) L. J. Smith, M. J. Sutcliffe, C. Redfield and C. M. Dobson, *Biochemistry*, 1991, **30**, 986; (*b*) T. Szyperski, P. Güntert, G. Otting and K. Wüthrich, *J. Magn. Reson.*, 1992, **99**, 552.
18 L. McIntyre and R. Freeman, *J. Magn. Reson.*, 1992, **96**, 425.
19 J.-M. Le Parco, L. McIntyre and R. Freeman, *J. Magn. Reson.*, 1992, **97**, 553.
20 J.-X. Havel and T. F. Havel, *J. Biomol. NMR*, 1994, **4**, 807.
21 J. Stonehouse and J. Keeler, *J. Magn. Reson. A*, 1995, **112**, 43.
22 USP 5 218 299/1993.
23 (*a*) J. H. B. Pease and D. E. Wemmer, in *Molecular Structures in Biology*, ed. R. Diamond, Oxford University Press, New York, 1993, p. 48; (*b*) D. Neuhaus, G. Wagner, M. Vasak, J. H. R. Kägi and K. Wüthrich, *Eur. J. Biochem.*, 1985, **151**, 257.
24 M. A. Karplus, *J. Am. Chem. Soc.*, 1963, **85**, 2870.
25 J. L. Marshall, *Methods in Stereochemical Analysis, Vol. 2: Carbon–Carbon and Carbon–Proton NMR Couplings*, Verlag Chemie, Florida, 1983.
26 I. O. Sutherland, *Ann. Rep. NMR Spectrosc.*, 1971, **4**, 71.
27 F. A. Carey and R. J. Sundberg, *Advanced Organic Chemistry, Part A: Structure and Mechanisms*, Plenum Press, New York, 1990, pp. 130–140 and references therein.
28 T. Robinson, in *Herbivores: their Interactions with Secondary Plant Metabolites*, eds. G. A. Rosenthal and D. H. Janzen, Academic Press, New York, 1979, pp. 413–448.
29 (*a*) Polygen Corp. 200 Fifth Ave., Waltham, MA 02254; (*b*) B. R. Brooks, R. E. Bruccoleri, B. D. Olafson, D. J. States, S. Swaminathan and M. J. Karplus, *J. Comput. Chem.*, 1983, **4**, 187.

Paper 5/02796I
Received 1*st May* 1995
Accepted 3*rd August* 1995